 DOI: 10.1002/masy.200750116

# PMMA Based Nanocomposites Filled with Modified $CaCO_3$ Nanoparticles

*Maurizio Avella, Maria Emanuela Errico, Gennaro Gentile**

**Summary:** PMMA based nanocomposites filled with calcium carbonate nanoparticles ($CaCO_3$) have been prepared by in situ polymerization approach. In order to improve inorganic nanofillers/polymer compatibility, PBA chains have been grafted onto $CaCO_3$ nanoparticle surface. Morphological analysis performed on nanocomposite fractured surfaces has revealed that the $CaCO_3$ modification induces homogeneous and fine dispersion of nanoparticles into PMMA as well as strong interfacial adhesion between the two phases. Mechanical tests have shown that both unmodified and modified $CaCO_3$ are responsible for an increase of the Young's Modulus, whereas only PBA-grafted nanoparticles allow to keep unchanged impact strength, strongly deteriorated by adding unmodified $CaCO_3$. Finally, the presence of $CaCO_3$ nanoparticles significantly improves the abrasion resistance of PMMA also modifying its wear mechanism.

**Keywords:** compatibilization; interfaces; mechanical properties; nanocomposites; structure-property relations

## Introduction

Poly(methylmethacrylate), PMMA, is an important technopolymer finding application in many sectors such as aircraft glazing, signs, lighting, architecture, and transportation. Moreover, since PMMA is non-toxic, it could be also useful in dentures, medicine dispensers, food handling equipments, throat lamps, and lenses. Unfortunately, PMMA is characterized by poor abrasion resistance with respect to glass, thus limiting its potential use in other fields. Despite several efforts, attempts to improve the PMMA scratch resistance have induced other drawbacks, such as a decrease of the impact strength.

It is well known that the incorporation of inorganic nanoparticles into polymers can provide high performance materials. Improved and unexpected properties can be achieved owing to the enormous interfacial adhesion region characteristic of nanoparticles.[1–6]

As a result of the large surface area of nanofillers, significantly smaller amounts of particles (1–5% by weight) compared to conventional microfillers (10–50% by weight) can induce dramatic changes in host matrix properties thus obtaining materials characterized by a lower density and a better processability.

The main goal of this research was to improve PMMA abrasion resistance preserving its mechanical properties. As a matter of fact, PMMA based nanocomposites filled with calcium carbonate nanoparticles ($CaCO_3$) were prepared. Previous researches focused on the preparation of polymer based nanocomposites have shown that properly modified $CaCO_3$ nanoparticles are competitive in respect to other inorganic nanofillers, such as SiC, to impart extraordinary properties to thermoplastic materials (polyolefins, polyesters, polyacrylates, polyamides) without strongly affecting the production costs.[7–12]

Istituto di Chimica e Tecnologia dei Polimeri del CNR, Via Campi Flegrei, 34 – 80078 Pozzuoli (NA) – Italy
E-mail: gengenti@ictp.cnr.it

In order to promote polymer/nanofillers interfacial adhesion, poly(butylacrylate) (PBA) chains were grafted onto $CaCO_3$ surface. This choice depends either from the necessity of improving the compatibility between organic and inorganic phase such as the nanoparticle dispersion or from the possibility of transferring the elastic property of the surface modifier to nanocomposites through the interfacial region, by exploiting the high specific surface area of nanofillers. Moreover, nanocomposites containing unmodified nanoparticles were also prepared in order to verify the role of the surface modifier on the nanofiller dispersion and on final properties of materials.

## Experimental Part

### Materials

Methylmethacrylate (MMA), butylacrylate (BA), dibenzoylperoxide (DBPO), vinyltrimethoxysilane (VTMS), KI, ICl, $Na_2S_2O_3$ 0.1 M solution, Aldrich reagent-grade product, were used without further purification.

Precipitated uncoated $CaCO_3$ nanoparticles (spherical shape, 70 nm average diameter) were kindly supplied by Solvay Advanced Functional Minerals (Giraud-France).

### $CaCO_3$ Surface Modification

A silane coupling agent (VTMS) was used to introduce double bonds (i.e., reactive groups) onto the surface of $CaCO_3$ nanoparticles. 9 g of $CaCO_3$ and 0.45 g of VTMS were suspended in 210 mL of 95% ethyl alcohol solution. The mixture was refluxed at the ethanol boiling temperature ($\sim 85\,^{\circ}C$) for 12 h under mechanical stirring. After that, the nano-$CaCO_3$ particles were centrifuged, and the precipitate was extracted with ethyl alcohol for 16 h to remove the unreacted silane. Then the silanized nano-$CaCO_3$ (S-$CaCO_3$) were dried at $80\,^{\circ}C$ under vacuum for 24 h.

In a flask 9 g of S-$CaCO_3$were dispersed into 70 mL of chloroform in an ultrasonic bath for 20 min at room temperature. Then the flask was heated at $80\,^{\circ}C$ in a oil bath and a solution of 3.6 g of BA containing 0.036 of DBPO was added dropwise. The reaction was carried out for 12 h under mechanical stirring. The final product (unextracted PBA-$CaCO_3$) was recovered after solvent evaporation and dried overnight at $100\,^{\circ}C$ under vacuum. Then, the ungrafted PBA was removed by Soxhlet extraction with chloroform for 16 h. Finally, the recovered PBA-g-$CaCO_3$ phase was dried at $80\,^{\circ}C$ overnight.

### PMMA/$CaCO_3$ Preparation

In a flask 0.5 g (1.5 g) of PBA-g-$CaCO_3$ were added to 49.5 g (48.5 g) of MMA. The dispersion was kept for 20 min in an ultrasonic bath. After this period, 1% by weight of DBPO (with respect to the acrylic phase) was added to the dispersion and then the flask was heated in an oil bath at $80\,^{\circ}C$. The dispersion was mechanically stirred until a critical viscosity corresponding to a prepolymerization step of the monomer. The viscous mixture was then poured into a mould and kept at $70\,^{\circ}C$ for 12 h in oven. Finally, the temperature was raised to $140\,^{\circ}C$ for further 12 h to complete the polymerization process. This preparation procedure was also used for uncoated nanoparticles, as well as for neat PMMA.

### Techniques

The content of double bonds introduced onto the $CaCO_3$ surface was detected by titration, according the following procedure: 0.5 g of S-$CaCO_3$, 50 mL of chloroform, and 20 mL of ICl solution in acetic acid (0.1 M) were poured into a 150-mL flask. After stirring for 15 min, 20 mL of KI solution (15%) were charged. Then the mixture was titrated with 0.1 M $Na_2S_2O_3$ solution (volume $V_1$). The same experiment was repeated with unmodified $CaCO_3$ nanoparticles, and the necessary volume of the $Na_2S_2O_3$ solution used for this titration is $V_o$. Then, the amount of double bonds ($n_{VTMS}$) was calculated by the following equation:

$$n_{VTMS} = 0.5 \times (V_0 - V_1) \times 0.1 \quad (1)$$

 

where $V_0$ and $V_1$ are expressed in liters and 0.1 is the $Na_2S_2O_3$ solution concentration (mol/L).

Infrared spectra were recorded at room temperature using 64 scans, 2 $cm^{-1}$ resolution with a Perkin Elmer Paragon 2000 Fourier Transform Infrared (FTIR) spectrometer. FTIR analysis was performed on pressed disc obtained by mixing samples (uncoated $CaCO_3$, unextracted PBA-$CaCO_3$ and PBA-g-$CaCO_3$) with KBr powder.

Thermogravimetric analysis (TGA) was performed on neat $CaCO_3$, S-$CaCO_3$, unextracted PBA-$CaCO_3$ and PBA-g-$CaCO_3$-nanoparticles by using a Perkin Elmer Pyris Diamond TG/DTA, by recording the weight loss as a function of temperature. The samples were heated from 40 °C to 1100 °C at a scanning rate of 10 °C/min in air atmosphere. The amount of PBA grafted onto $CaCO_3$ surface (PBA-g-$CaCO_3$) was evaluated by comparing the related TGA traces with that of S-$CaCO_3$.

Glass transition temperatures (Tg) were evaluated by using a differential scanning calorimeter Mettler DSC-30. The samples were heated from −100 to 200 °C at a scanning rate of 20 °C/min. Dry nitrogen gas was purged through the cell. The Tg was determined for each sample as the temperature corresponding to the maximum of the peak obtained by the first order derivative trace of the DSC thermoanalytical curve.

Morphological analysis was performed by using a scanning electron microscope (SEM), Cambridge Stereoscan microscope model 440, on cryogenically fractured surfaces and on nanocomposite surface after abrasion tests. Before the observation, samples were metalled with a gold layer.

Flexural tests were carried out at room temperature by using an Instron mechanical testing instrument (Model 1122). The test span was 48 mm. The cross-head speed was 1 mm/min. The elastic modulus (E) was measured on unnotched samples (60 mm long, 6.0 mm wide, 3.0 mm thick). The critical stress intensity factor ($K_c$) and the critical strain energy release rate ($G_c$) were calculated according to the concepts of linear elastic fracture mechanics (LEFM) on samples (60 mm long, 10.0 mm wide, 3.0 mm thick) sharply notched as following described: first a blunt notch (about 2 mm deep) was obtained through a machine with a V-shaped tool and then a sharp notch 0.2 mm deep was made by a razor blade. The final value of the notch depth was measured after fracture by an optical microscope.[13,14]

Abrasion tests were carried out using a Taber abrader model 5130 on neat PMMA, PMMA/$CaCO_3$ and PMMA/PBA-g-$CaCO_3$ materials. The dimensions of specimens were 5 cm × 10 cm × 10 cm. The abrasive paper, 80 grain, was applied on Teflon rollers of the machine. The applied weight of the arms was 1000 g. Three sessions of 500 cycles were performed on samples. The abrasion resistance was evaluated as the weight loss of samples. The above described experimental procedure was performed on all prepared samples in order to evaluate the abrasion resistance of materials.

## Results and Discussion

In order to improve polymer/inorganic nanofiller compatibility, PBA chains were grafted onto $CaCO_3$ nanoparticle surface. The choice of the surface modifier derives either from the necessity of improving the homogeneity of the nanoparticle dispersion into the matrix or from the objective of transferring the elastic property of the surface modifier to the nanocomposites through the interfacial region.

In particular, the surface modification was carried out in two steps. In the first, a double bonds endcapped silane agent, vinyltrimethoxysilane (VTMS), was added to an alcoholic solution in which nanoparticles were previously dispersed to introduce reactive groups (i.e. double bonds) onto nanoparticle surface. After the reaction, the excess of the silane agent was removed by Soxhlet extraction. The amount of grafted silane, determined by titration, was about 1.3% by weight with respect to dried nanoparticles.

In the second step BA phase, ratio BA/$CaCO_3$ 0.4/1 by weight, was polymerized by

 

thermal decomposition of an organic peroxide (DBPO) in presence of endcapped double bonds silane modified nanoparticles (S-$CaCO_3$) in order to graft polyacrylic chains onto nano-$CaCO_3$ (PBA-g-$CaCO_3$).

In fact, the vinyl groups onto $CaCO_3$ surface are able to react with radical species, such as growing acrylic macroradicals. As a matter of fact, during the radical PBA polymerization, reactions of chain transfer and/or termination to the PBA phase, involving vinyl groups of $CaCO_3$ surface, become statistically possible giving the above described PBA-g-$CaCO_3$ grafted species.

After the extraction of ungrafted PBA homopolymer, FTIR spectroscopy was carried out on modified nanopowders, see Figure 1.

As it can be observed, the insurgence of an absorption band centred at 1735 $cm^{-1}$ can be remarked in the spectra of unextracted modified nanoparticles, see Figure 1b. This band is assigned to PBA carbonyl groups. After extraction of PBA homopolymer, this band is still evident (see Figure 1c) confirming the grafting reaction of PBA onto nanofiller surface.

The amount of grafted PBA was determined by thermogravimetric analysis (TGA) performed on extracted PBA-g-$CaCO_3$ nanoparticles by measuring the weight loss of the grafted organic phase. This analysis permitted to evaluate that the nanoparticle surface was grafted by about 5% by weight of the polyacrylic phase.

DSC analysis was also performed on the PBA-g-$CaCO_3$ nanoparticles and it under-

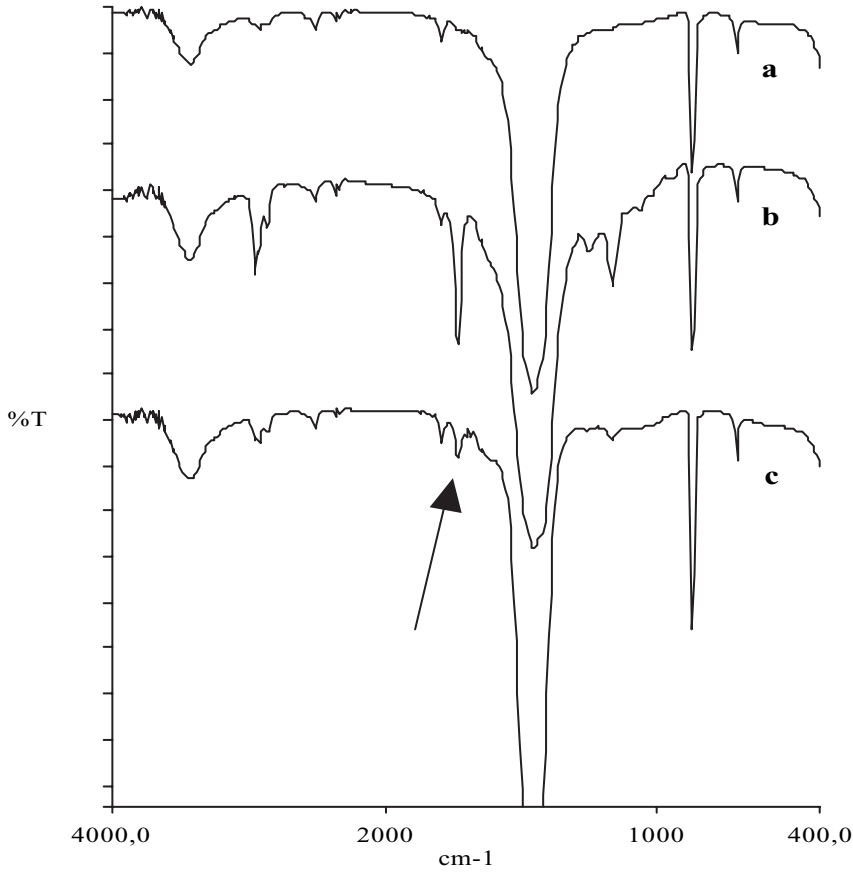


***Figure 1.***
FTIR spectra of: a) neat $CaCO_3$ nanoparticles; b) unextracted PBA-$CaCO_3$; c) extracted PBA-g-$CaCO_3$.

 

lined a strong increase (about 15 °C) of the $T_g$ value relative to the PBA phase (−45 °C) compared to that of neat PBA (−60 °C). This shift can be attributed to the fact that the polyacrylic chains are anchored to the calcium carbonate surface thus reducing the PBA chain mobility and confirming the occurred grafting reaction.

### PMMA/$CaCO_3$ Nanocomposites

PMMA based nanocomposites filled with 1 and 3% by weight of PBA-g-$CaCO_3$ nanoparticles were prepared by in situ polymerization.

PBA-g-$CaCO_3$ were dispersed into MMA phase by premixing in an ultrasonic bath. Then, the polymerization was induced by thermal decomposition of DBPO (1 wt % with respect to MMA). As detailed described into the experimental session, the in situ polymerization process was carried out in two steps. During the first step, performed under mechanical stirring, the low mixture viscosity favored the fine nanoparticle dispersion. Then, during the polymerization process, the growing PMMA chains contributed to increase the viscosity of the medium thus assuring the freezing of the obtained nanofiller dispersion. In the last step, performed in the oven, the PMMA polymerization was completed, as confirmed by the absence of an exothermic peak DSC curves, that would indicate a residual heat of polymerization. The same procedure was also used to prepare PMMA filled with 3% by weight of neat $CaCO_3$ in order to verify the influence of the coating agent on final nanocomposite properties.

In order to evaluate the nanocomposite morphology and the interfacial adhesion between the two components, SEM analysis was performed on cryogenically fractured surfaces of samples. As an example, the micrographs of materials containing 3% by weight of unmodified and modified nanoparticles are reported in Figure 2. As shown, PBA-g-$CaCO_3$ (see Figure 2b) appear finely and homogeneously dispersed into PMMA matrix. Moreover a strong interconnection between the phases was also evidenced due to the absence of voids

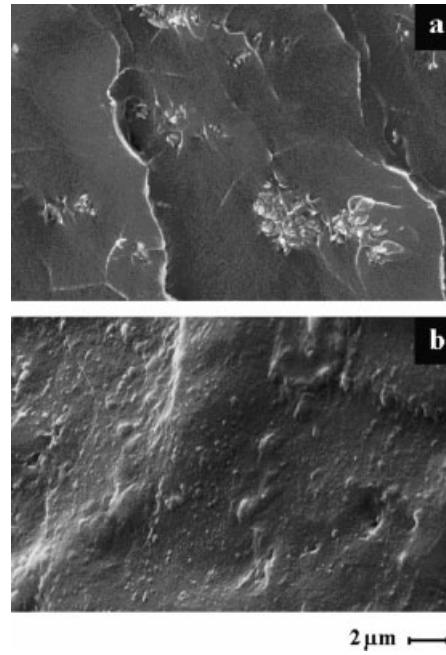


***Figure 2.***
SEM micrographs of fractured surface of: a) PMMA containing 3wt% of uncoated $CaCO_3$; b) PMMA containing 3wt% of PBA-g-$CaCO_3$.

and debonding phenomena between the two phases after the applied mechanical load. On the contrary, in the case of unmodified nanoparticles (see Figure 2a), some agglomeration phenomena are clearly evident. This analysis permitted to assess that nanoparticle modification allow the improvement of the PMMA/$CaCO_3$ compatibility. This is considered to be due to the fact that grafted polyacrylic chains on the surface increase the affinity of nanoparticles towards polymeric matrix, thus reducing the tendency of particles towards aggregation phenomena and consequently improving the interfacial adhesion between the two phases in the nanocomposite.

Mechanical parameters of PMMA and PMMA based nanocomposites were evaluated by flexural tests on unnotched (Young's Modulus) and notched samples ($K_c$ and $G_c$). Results are reported in Table 1. As resumed, both uncoated and coated nanoparticles increase the Young's Modulus of PMMA up to about 20%.

 

*Table 1.*
Results of flexural tests carried out on unnotched (Young's Modulus) and notched ($K_c$ and $G_c$) samples of PMMA and PMMA based nanocomposites.

| Sample | Young's Modulus (MPa) | $K_c$ (MN/m$^{3/2}$) | $G_c$ (kJ/m$^2$) |
|---|---|---|---|
| PMMA | 2197 | 1.17 | 0.60 |
| PMMA/$CaCO_3$ 3% | 2574 | 0.99 | 0.42 |
| PMMA/PBA-g-$CaCO_3$ 1% | 2445 | 1.22 | 0.68 |
| PMMA/PBA-g-$CaCO_3$ 3% | 2520 | 1.18 | 0.62 |

Generally speaking, the inclusion of a rigid filler into polymeric matrix results in a heterogeneous system. These heterogeneities could act as stress concentration points when an external mechanical load is applied thus assuring the increase of mechanical performances of the material.

The relevance of this phenomenon is strictly related to geometry and size of fillers and essentially to the interaction between fillers and polymeric matrix. As a matter of fact, very high improvements of mechanical properties (up to 50%) can be recorded in the case of rigid nanofillers homogeneously dispersed into polymer.[15,16]

The slight increase obtained in this case can be explained taking into account that, for uncoated nanoparticles, clustering phenomena reduce the extent of the interfacial region between filler and matrix and consequently the mechanical improvement that could be obtained, in principle, by the incorporation of rigid nanoparticles into PMMA.

As concerns nanocomposites filled with PBA-g-$CaCO_3$ nanoparticles, although nanoparticles appear finely dispersed and well welded to PMMA, the presence of the rubbery coating onto $CaCO_3$ surface partially damps the effects of the rigid filler on the material stiffness.

Finally, the toughness of nanocomposites was also evaluated at low deformation rate. It is generally accepted that the presence of a rigid filler could deteriorate the toughness of polymeric matrix while a rubbery phase could substantially improve this property.[17]

As a matter of fact, in this research the grafting of PBA onto nanoparticle surface was performed to mitigate the possible negative effect attributable to the rigid filler on this parameter. As shown in Table 1, while the presence of uncoated nanoparticles significantly reduces $K_c$ and $G_c$ values with respect to neat PMMA, PBA-coated nanoparticles seem to keep unchanged these parameters.

The above findings prompted us in the future work to graft higher amount of the rubbery phase onto nanoparticle surface in order to raise the toughness of PMMA based nanocomposites.

In Table 2, results of abrasion tests are summarized. The presence of nanoparticles strongly increases abrasion resistance of PMMA. In fact, an improvement of this property up to 50%, was recorded even at low nanoparticle content and independently from the presence of the coating agent. The abrasion resistance of a solid is defined as its ability to withstand the progressive removal of material from its surface as a result of mechanical action of rubbing, scraping, or erosion.[18] Therefore, this significant improvement can be explained considering that nanoparticles support part of the applied load and, in this way, the penetration into the polymer is reduced. Moreover, as reported in Figure 3a, the wear mechanism of neat PMMA occurs via microcracking phenomena defining it as a brittle and a low abrasion resistance material.

*Table 2.*
Abrasion test results of neat PMMA and PMMA-based nanocomposites, measured as weight loss.

| Sample | Weight loss (mg/cm$^2$) |
|---|---|
| PMMA | 42.0 |
| PMMA/$CaCO_3$ 3% | 20.2 |
| PMMA/PBA-g-$CaCO_3$ 1% | 26.6 |
| PMMA/PBA-g-$CaCO_3$ 3% | 20.5 |

 

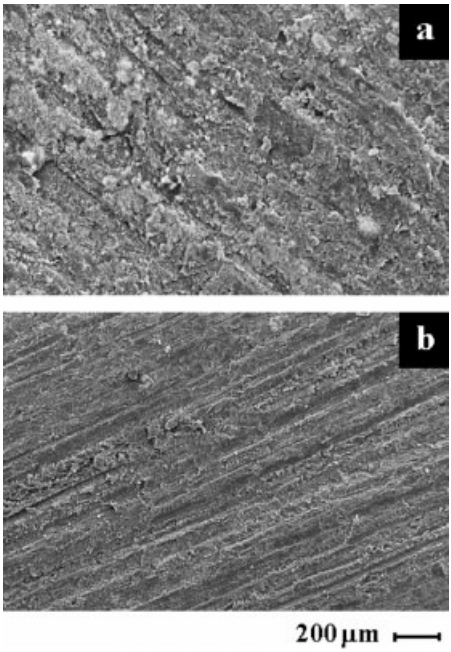


***Figure 3.***
SEM micrographs of the nanocomposites surface after abrasion test of: a) PMMA; b) PMMA containing 3wt % of $CaCO_3$.

On the other hand, the presence of nanoparticles induces only microcutting and/or microploughing phenomena thus generating a plastic deformation and consequently an increase of the abrasion resistance (see Figure 3b, representative of all the nanocomposites containing 3wt% of either uncoated or modified nanoparticles).

## Conclusions

PMMA based nanocomposites filled with unmodified and PBA-modified calcium carbonate nanoparticles were prepared by in situ polymerization. Morphological analysis of cryogenically fractured surfaces allowed to assess that the grafting of PBA onto nanoparticle surface induces a strong interconnection between the phases and homogeneous and fine dispersion of nanoparticles into the matrix. Mechanical analysis underlined that the presence of the rubbery phase permits an improvement of the Young's Modulus of PMMA without negatively influencing its toughness, whereas unmodified nanoparticles are responsible for a significant deterioration of both $K_c$and $G_c$ parameters. Finally, both neat and modified $CaCO_3$ nanoparticles strongly increase the abrasion resistance of PMMA, independently from the presence of the coating agent.

[1] M. D. Morse, *Chem. Rev.* **1986**, *86*, 1049.
[2] W. P. Halperin, *Rev. Mod. Phys.* **1986**, *58*, 533.
[3] A. Henglein, *Chem. Rev.* **1989**, *89*, 1861.
[4] G. D. Stucky, J. E. MacDougall, *Science* **1990**, *247*, 669.
[5] V. Kresin, *Phys. Rep.* **1992**, *220*, 1.
[6] X. Cao, Y. Koltypin, R. Prozorov, G. Katabi, A. Gedanken, *J. Mater. Chem.* **1997**, *7*, 2447.
[7] C. M. Chan, J. Wu, X. Li, Y. K. Cheung, *Polymer* **2002**, *43*(10), 2981.
[8] M. L. Di Lorenzo, M. E. Errico, M. Avella, *J. Mater. Sci.* **2002**, *37*(11), 2351.
[9] M. Avella, M. E. Errico, E. Martuscelli, *Nanoletters* **2001**, *1*(4), 213.
[10] M. Avella, S. Cosco, M. L. Di Lorenzo, E. Di Pace, M. E. Errico, G. Gentile, *Macr. Symp.* **2006**, *234*, 156.
[11] M. Avella, M. E. Errico, G. Gentile, *Macr. Symp.* **2006**, *234*, 170.
[12] M. Avella, C. Carfagna, P. Cerruti, M. E. Errico, G. Gentile, *Macr. Symp.* **2006**, *234*, 163.
[13] K. Friedrich, "*Application of Fracture Mechanics to Composite Materials*", Elsevier, Composite Materials Series Vol. *6*, New York **1991**.
[14] J. C. Williams, "*Fracture Mechanics of Polymers*", John Wiley & Sons, New York **1984**.
[15] G. M. Kim, D. H. Lee, B. J. Hoffmann, G. Stoppelmann, *Polymer* **2001**, *42*, 1095.
[16] T. S. Creasy, Y. S. Kang, J. Thermoplas. *Compos. Mater.* **2004**, *17*, 205.
[17] M. Abbate, E. Martuscelli, P. Musto, G. Ragosta, *Die Ang. Makr. Chem.* **1997**, *246*, 23.
[18] H. Czichos, "Introduction to Friction and Wear" in "*Friction and Wear of Polymer Composites*", K. Friedrich, Ed., Elsevier, New York **1986**, p. 1.

 